Validation of the V5 MODIS Land-Surface Temperature Product Worldwide

Zhengming Wan, ICESS, University of California, Santa Barbara, CA (wan@icess.ucsb.edu)

Institute for Computational Earth System Science, University of California, Santa Barbara

1. Radiance-based Validation of the V5 MODIS LST Product Worldwide at 26 new sites

Site	Location	Latitude, Longitude (°)	Landcover Type	MOD11 or MYD11_L2	type of atmospheric profiles	mean (std) of LST errors (K) **
11	Recife, Brazil	7.96 S, 34.94 W	evergreen forest (2)	MOD11	radiosonde	0.4 (0.4)
12	Moree, Australia	29.555 S, 149.86 E	open shrubland (7)	MOD11	radiosonde	-0.6 (0.4)
13	Port Elizabath, S. Africa	33.95 S, 23.59 E	evergreen forest (2)	MYD11	radiosonde	-0.4 (0.3)
14	WLT Alert, Canada	82.4 N, 62.33 W	shrubland (7)/snow (15)	MOD11	radiosonde	0.2 (0.6)
15	South Pole	89.95 S, 0.05 E	snow/ice (15)	MOD11	radiosonde	-0.5 (0.6)
16	McMurdo, Antarctica	77.75 S, 164.1 E	snow/ice (15)	MOD11	radiosonde	0.1 (0.3)
17	Dye-2, Greenland	66.481 N, 46.28 W	snow/ice (15)	MOD11	NCEP	0.0 (0.5)
18	Summit, Greenland	72.58 N, 38.475 W	snow/ice (15)	MOD11	NCEP	0.1 (0.5)
19	Cherskij, Russia	68.75 N, 161.27 E	Snow (15)/shrubland (7)	MOD11	radiosonde	0.0 (0.5)
20	Gaze, Tibet	32.3 N, 84.06 E	open shrubland (7)	MOD11	NCEP	-0.6 (0.2)
21	Hainich, Germany	51.079 N, 10.452 E	mixed forest (5)	MOD/MYD	radiosonde	-0.2 (0.5)
22	Paris, France	48.8 N, 2.35 E	urban (13)	MYD11	radiosonde	0.1 (0.4)
23	near Paris, France	48.45 N, 2.25 E	cropland (12)	MYD11	radiosonde	0.0 (0.6)
24	Nimes, France	43.84 N, 4.37 E	urban (13)	MYD11	radiosonde	0.1 (0.5)
25	near Nimes, France	43.828 N, 4.535 E	cropland (12)	MYD11	radiosonde	-0.1 (0.6)
26	Milan, Italy	45.485 N, 9.21 E	urban (13)	MYD11	radiosonde	-0.3 (0.7)
27	near Milan, Italy	45.297 N, 9.26 E	cropland (12)	MYD11	radiosonde	-0.3 (0.6)
28	Cuneo, Italy	44.53 N, 7.62 E	cropland (12)	MYD11	radiosonde	0.0 (0.5)
29	Payerne, Switzerland	46.855 N, 6.965 E	cropland (12)	MYD11	radiosonde	-0.1 (0.5)
30	Nenjiang, China	49.07 N, 125.23 E	cropland (12)/snow (15)	MOD11	radiosonde	-0.3 (0.6)
31	Yichun, China	47.76 N, 128.88 E	mixed forest (5)	MOD11	radiosonde	0.1 (0.6)
32	Harbin, China	45.73 N, 126.65 E	urban (13)	MOD11	radiosonde	0.2 (0.4)
33	near Harbin, China	45.9 N, 127.1 E	cropland (12)	MOD11	radiosonde	0.3 (0.5)
34	Farafra, Egypt	27.04 N, 27.97 E	bare soil (16) in desert	MYD11	radiosonde	0.9 (0.2)
35	SVU, Egypt	26.285 N, 32.78 E	bare soil (16) in desert	MYD11	radiosonde	-1.6 (0.4)
36	In-salah, Algeria	27.18 N, 2.6 E	bare soil (16) in desert	MOD/MYD	radiosonde	-3.2 (0.5)

** after applying the $\delta(T_{31}-T_{32})$ correction method.

At least one site in each continent. LST errors span in a wide range & large LST errors exist only at desert sites.

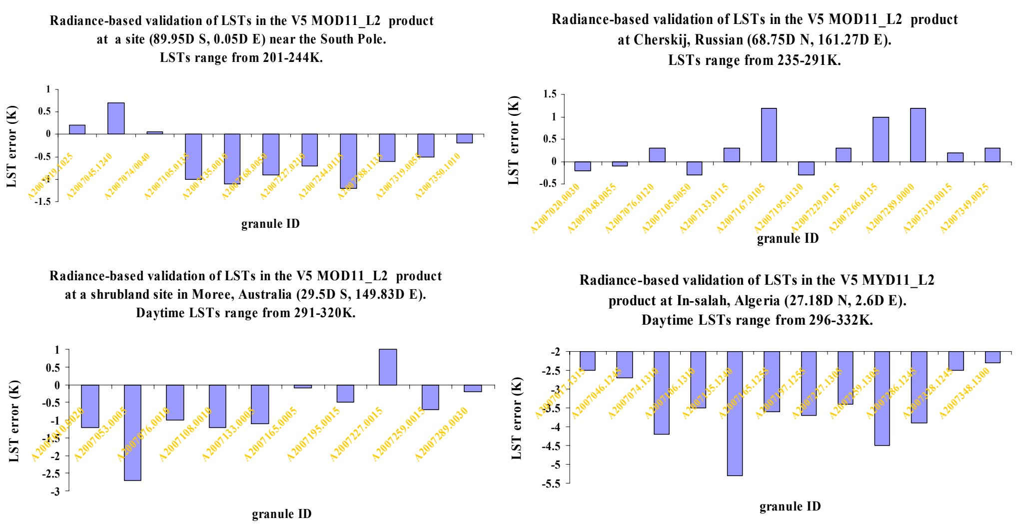

Fig. 1, LST errors at R-based validation sites near the South Pole, Cherkij Russia, Moree Australia, and In-salah Algeria.

2. Major Problems in the V5 MODIS LST Product

1) The split-window algorithm significantly underestimates daytime LSTs when LST > Ts-air + 16K and cwv > 1.5cm (in bare soil areas) because the high LST values in these conditions were not considered in the development of the split-window algorithm. This problem can be resolved in the V6 algorithm.

2) There may be large errors in the LSTs retrieved by the split-window algorithm in desert regions because of the large uncertainties in the classification-based emissivity values. This problem cannot be resolved in the V6.

3) Because the day/night algorithm is tightly bounded with the split-window algorithm in V5, the large errors in LSTs retrieved by the split-window method in desert regions also affect the day/night algorithm. So we need to tune the day/night algorithm and make it work better even when the split-window algorithm does not work well. It is possible to make a significant improvement in the V6 day/night algorithm.

3. New Improvements for the C6 (V6) MODIS LST Product

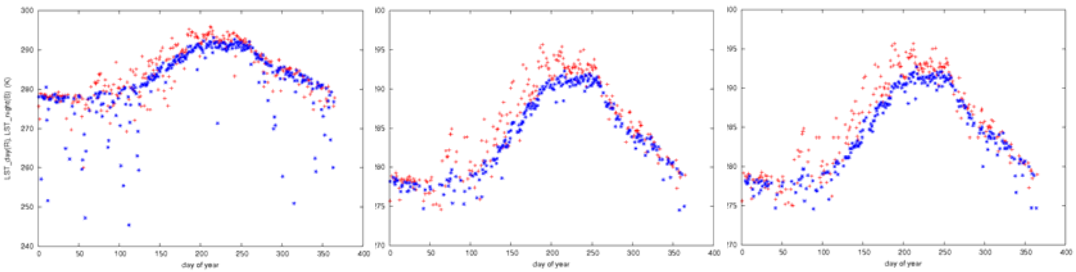

Fig. 2, LST_day (red) and LST_night (blue) at Lake Tahoe, CA, retrieved by the day/night algorithm in the MYD11B1 product in 2007 in C41 (left), C5 (middle) and C6 (right). Note that Lake Tahoe does not freeze in the whole year so the low LST values in the C41 are due to cloud contaminations.

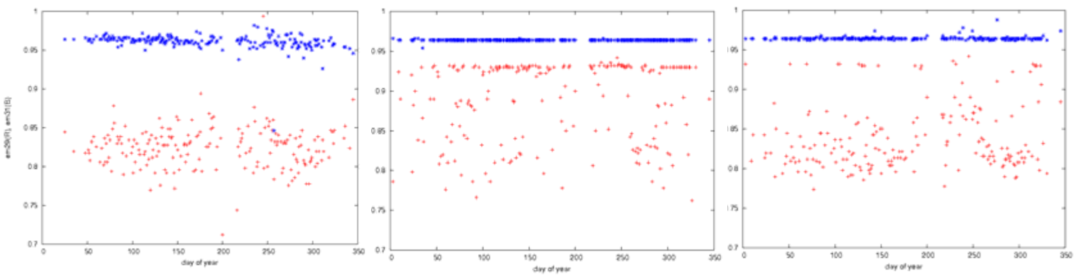

Fig. 3, em29 (red) and em31 (blue) at Imperial sand dunes, CA, retrieved by the day/night algorithm in MYD11B1 product in 2007 in C41 (left), C5 (middle) and C6 (right). Some emissivity values in the C41 are too low (corresponding to unreasonably high LSTs). In C5 there are too many days with em29 values near 0.93 (corresponding to lower LSTs).

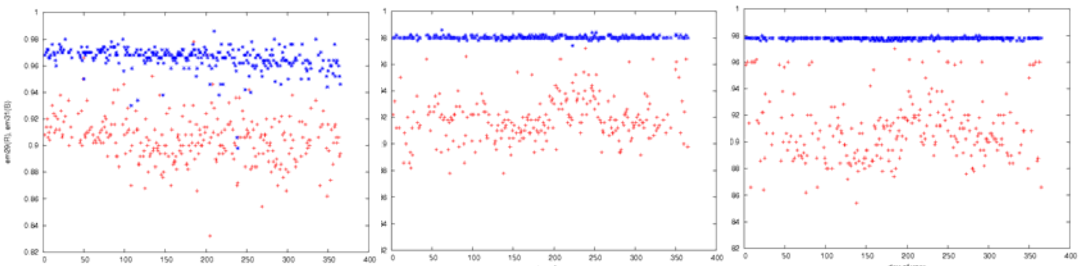

Fig. 4, em29 (red) and em31 (blue) at a shrubland in Mojave, CA, retrieved by the day/night algorithm in MYD11B1 product in 2007 in C41 (left), C5 (middle) and C6 (right). Many emissivity values in the C41 are too low, which would correspond to unreasonably high LSTs.

Wan, Z., (2008). New refinements and validation of the MODIS land-surface temperature/emissivity products. *Remote Sensing of Environment*, 112, 59-74.
Wan, Z., & Li, Z.-L., (2008). Radiance-based validation for the V5 MODIS land-surface temperature product. *International Journal of Remote Sensing*, 29, 5373-5395.
Coll, C., Wan, Z., & Galve, J.M., (2009). Temperature-based and radiance-based validation for the V5 MODIS land-surface temperature product. *JGR*, 114, D20102, doi:10.1029/2009JD012038.